

Wireless RF communication in biomedical applications

Inke Jones^{1,2,3}, Lucas Ricciardi^{1,2}, Leonard Hall^{1,2},
Hedley Hansen⁴, Vijay Varadan⁵, Chris Bertram⁶,
Simon Maddocks⁷, Stefan Enderling^{1,2,8}, David Saint^{1,9},
Said Al-Sarawi^{1,2} and Derek Abbott^{1,2}

¹ Centre of Biomedical Engineering, University of Adelaide, SA 5005, Australia

² Department of Electrical and Electronic Engineering, University of Adelaide, SA 5005, Australia

³ Department of Biomedical Engineering, University of Applied Sciences, D-45877 Gelsenkirchen, Germany

⁴ DSTO, EWD, PO Box 1500, Edinburgh, SA 5111, Australia

⁵ Research Center for the Engineering of Electronic and Acoustic Materials, Pennsylvania State University, University Park, PA 16802, USA

⁶ Graduate School of Biomedical Engineering, University of New South Wales, NSW 2052, Australia

⁷ Department of Animal Science, University of Adelaide, Roseworthy Campus, Roseworthy, SA 5371, Australia

⁸ Department of Electronics and Electrical Engineering, University of Edinburgh, Edinburgh EH9 3JF, UK

⁹ Department of Physiology, University of Adelaide, SA 5005, Australia

E-mail: ijones@eleceng.adelaide.edu.au and dabbott@eleceng.adelaide.edu.au

Received 5 September 2007, in final form 14 December 2007

Published 17 January 2008

Online at stacks.iop.org/SMS/17/015050

Abstract

This paper focuses on wireless transcutaneous RF communication in biomedical applications. It discusses current technology, restrictions and applications and also illustrates possible future developments. It focuses on the application in biotelemetry where the system consists of a transmitter and a receiver with a transmission link in between. The transmitted information can either be a biopotential or a nonelectric value like arterial pressure, respiration, body temperature or pH value. In this paper the use of radio-frequency (RF) communication and identification for those applications is described. Basically, radio-frequency identification or RFID is a technology that is analogous to the working principle of magnetic barcode systems. Unlike magnetic barcodes, passive RFID can be used in extreme climatic conditions—also the tags do not need to be within close proximity of the reader. Our proposed solution is to exploit an exciting new development in making circuits on polymers without the need for battery power. This solution exploits the principle of a surface acoustic wave (SAW) device on a polymer substrate. The SAW device is a set of interdigitated conducting fingers on the polymer substrate. If an appropriate RF signal is sent to the device, the fingers act as microantennas that pick up the signal, and this energy is then converted into acoustic waves that travel across the surface of the polymer substrate. Being a flexible polymer, the acoustic waves cause stresses that can either contract or stretch the material. In our case we mainly focus on an RF controllable microvalve that could ultimately be used for fertility control.

1. Introduction

Future MEM (microelectromechanical) systems will require the integration of active as well as passive devices. There

are many types of devices produced for different tasks, for example microchannels, micropumps and microvalves. These microstructures (e.g. microfluidic) are divided into two different categories: passive devices (without an actuator) and

active devices (with an actuator). Passive microvalves get their activating energy from the surrounding fluid and flow in only one direction is possible. On the other hand, the energy of active valves is externally supplied. The advantage of using active valves is that the control of very small sample volumes is possible, which is very important in biomedical, chemical, drug delivery and printing applications. They have a small dead volume that allows greater efficiency and makes a fast response time possible. Designs that do not unnecessarily heat the surrounding medium are possible [1]. The right choice of actuating principle is dependent on the structural dimensions, the technology, the response time, the force or torque as a function of displacement and the maximum power as well. Force can be generated using two main principles:

- (i) external forces are generated in the space between stationary and moving parts using thermopneumatic and electromechanical effects, electrostatic and magnetic fields or
- (ii) inner forces that use special materials having intrinsic actuation capabilities including piezoelectric, thermomechanical, shape memory, electro- and magnetostatic effects.

The main principles used for microvalves which have been successfully realized and implemented in industrial applications or prototypes are electromagnetic, thermodynamic, thermopneumatic and shape memory [2–10]. In our case the converse piezoelectric effect is used to control the microvalve. Because of surface acoustic wave (SAW) devices, new possibilities in controlling and processing electrical signals have been found. We will present the restrictions we face on antenna size and transmitter power and suggest a minimum suitable size for the internal antenna over the frequency range of 100 MHz–100 GHz, with regard to a microvalve consisting of a biocompatible silicone-based polymer with piezoelectric properties. This microvalve can potentially be used for different applications, e.g. fertility control, flow cytometry, drug delivery and DNA sequencing.

2. Piezoelectric effect

Piezoelectricity, discovered in 1880 by the brothers Jacques and Pierre Curie, is defined as a change in electrical polarization resulting from a change in applied stress, which is usually referred to as the direct piezoelectric effect. It can be utilized for the localization of devices in inaccessible places. The converse piezoelectric effect is a reciprocal effect where there is a change in strain for a free crystal (or stress for a clamped system) resulting from a change in applied field. Thus, the converse piezoelectric effect is typically used when a material is used as an actuator: input is a voltage gradient and output a strain. For low fields, there is a linear relationship between strain and electrical field. Reversing the field also reverses the direction of the strain [11]. A piezoelectric material has the characteristic of being elastic and generating an electric field when a force is applied to it and vice versa. Wave propagation on the surface of the piezoelectric material can thus be launched and detected by metal electrodes on the

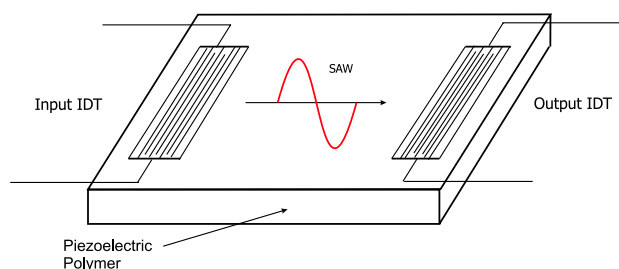


Figure 1. This figure shows a standard Rayleigh surface acoustic wave device with its input and output IDTs, and the propagation of the surface acoustic waves.

(This figure is in colour only in the electronic version)

surface of the material. There are currently many substrates in use for SAW devices. The most commonly used are lithium niobate, quartz and lithium tantalate, which are cut at various angles to the crystalline axes. In our case a piezoelectric polymer is used to activate the microvalve.

3. SAW devices

Surface acoustic wave (SAW) devices are recognized for their versatility and efficiency in controlling and processing electrical signals. They are based on propagation of acoustic waves in elastic solids and the coupling of these waves to electric charge signals via electrodes deposited on a piezoelectric material. Basically, we may think of a SAW device as consisting of a solid substrate with an input and output transducer. Because of this interdigital transducers (IDT) provide a practical method for generating and detecting surface acoustic waves. The input transducer converts the incoming signal by the inverse piezoelectric effect into acoustic waves, which propagate along the planar surface of the solid. At the output transducer, the SAWs are reconverted to an electrical signal. A standard Rayleigh SAW device is shown in figure 1.

A fundamental property of the SAW device is its ability to act as a signal delay line. The relatively slow propagation velocity of the surface acoustic waves of typically 3500 m s^{-1} allows delays of several microseconds on a small chip [14]. The phase velocity of the combined wave and the photolithographic resolution of the fabrication process determine the maximum sampling frequency of the transducers.

As an alternative to the use of a two-part SAW device, the receiving section can be replaced by a series of reflectors and the output identification device (ID tag) can be directly connected to a microstrip antenna to receive and transmit RF signals. The transmitted RF signal is received by the IDT antenna and transformed into a propagating surface acoustic wave. The response signals form a sequence of short pulses in accordance with the number and position of the reflectors on the crystal surface. The time delay of every partial response pulse depends on the SAW propagation velocity, which is affected by several physical quantities (temperature, pressure and strain) and the distance between the IDT and the reflectors [15]. The response signal is reflected to the IDT

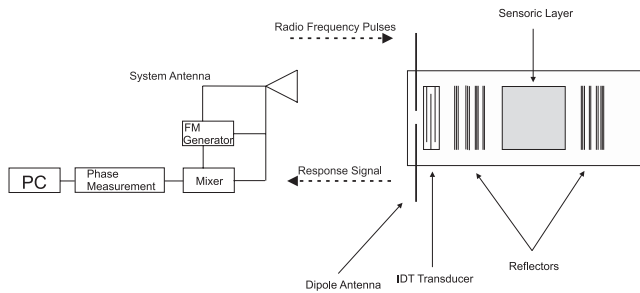


Figure 2. This figure shows the principle of a wireless SAW ID tag which uses reflectors on its surface instead of an output IDT to reflect the SAWs back to the input IDT which is directly connected to the antenna. This antenna is able to receive as well as to transmit RF pulses. The figure also shows the reader/transmitter station with its system antenna. The reading system has a linear frequency modulated (FM) signal generator and the FM signals are transmitted by the system antenna.

and transduced back into electromagnetic waves. These waves are radiated by the antenna and received and evaluated by the reader station. So it is possible to get information about the localization of the device as well as the ability to control its function. The basic principle of a wireless SAW ID tag is shown in figure 2.

Today, mainstream integrated circuits tend to use silicon as the substrate material. However, there is now a new growing field in the area of polymer electronics. This field is moving rapidly now that researchers have successfully fabricated transistors on a polymer substrate. This new paradigm has the advantage that circuits can be flexible and lightweight. Also the material parameters of a polymer can be more finely tuned than in silicon [11]. A further advantage is that polymer materials are more bio-friendly for implantation in animals or the human body—this is attractive for a host of applications from artificial valves to pacemakers. Polymer materials can be flexed and textured, whereas silicon is hard and brittle. The active circuitry on a polymer can be elegantly encapsulated and isolated from body fluids and tissues. Electro-active polymers have increasingly become of interest, particularly ionic polymer metal composites (IMPCs) [12, 13]. IMPC-based actuators show very interesting properties for biomedical applications, such as low required voltage, high compliance and softness, but more research needs to be carried out to fully understand their working principle and to solve some potential drawbacks (the actuators require a humid environment) [13].

However, one problem with conventional transistor circuitry, even on polymers, is that transistors require a source of power, i.e. a battery. The number of useful biomedical applications would greatly increase if a battery was not needed. There are obvious disadvantages with implanting batteries into the body—as well as the problem of replacement, the extra mass means that it is only limited to special applications such as in pacemakers.

A possible solution is to use conventional radio-frequency identification device (RFID) technology where low power circuits can obtain their power from an electromagnetic field. However, there are problems here:

- (i) the resulting circuit size would be quite large for, say, application in male fertility control;

- (ii) fully integrated circuit technology on polymer is not mature enough yet; and
- (iii) there is no direct actuation mechanism in this type of technology.

Our solution therefore is to turn to polymer-based SAW devices.

4. Polymers in biomedical RFID

Biomedical RFID technology exploits the working principle of the piezoelectric effect, which is defined as a change in electrical polarization resulting from a change in applied stress, which is usually referred to as the direct piezoelectric effect. A piezoelectric material has the characteristic of being elastic and generating an electric field when a force is applied to it and vice versa. Wave propagation on the surface of the piezoelectric material can thus be generated and detected by interdigital transducers (IDTs) on the surface of the material.

When a voltage received from the antenna is applied to the terminals of the IDT it creates a potential difference across the busbar. Each pair of fingers can be regarded as a capacitor. Hence the potential difference creates charge on each finger, which is proportional to the applied voltage. The charge created causes a surface acoustic wave to be generated as a result of the piezoelectric effect. If we consider the first finger pair, the charge on the first finger creates a positive acoustic pulse and the charge on the second finger creates a negative pulse, hence creating an overall negative pulse. It can be seen that the second finger pair is connected to the busbar with an opposite sign to the first pair, so it will generate an overall positive pulse. It is clearly apparent that by ordering the fingers in certain ways we can affect the creation of acoustic pulses. This effect is exploited in coding the devices as will be explained in later sections.

It is clearly apparent the importance of having a device that can be encoded if successful *in vivo* applications are to become a reality. With today's technology we can achieve encoding of SAW devices by designing the IDT's fingers in a specific order. By designing the IDT fingers in such a way so that their polarity and orientation is related to the input code, we can ensure that only a correct acoustic wave propagates. This can be seen in figure 3. When a negative RF pulse is injected into the leftmost finger pair (pair 1), it excites a positive acoustic wave. We can see that the generated wave is opposite in sign to the injected pulse. This is due to the fact that the negative pulse injected into a negative finger pair cancels to be positive. For this reason we need the input code to be the equivalent to the finger pair configurations. The acoustic wave generated at the first finger pair will reach the receiving transducer at the same time as the wave from the second finger pair. Since these will be of the same sign and phase they will constructively interact to increase the size of the wave. From this we can see that, if the incorrect code is input to the system, the generated pulses will destructively interact. Hence, by increasing the number of finger pairs we can increase the number of possible codes, which makes it more secure for the patient—because that makes it harder to manipulate or abuse

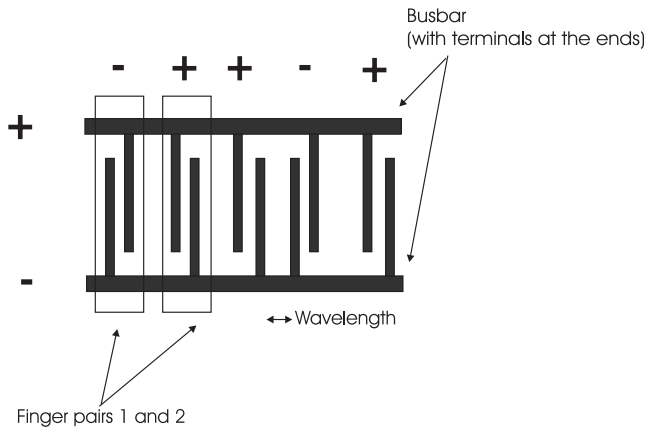


Figure 3. This figure shows the basic structure of an IDT and how it works. When a voltage is received from the antenna, which is directly connected to the IDT, this voltage is applied to the terminals of the transducer and creates a potential difference across the busbar. Each pair of fingers can be regarded as a capacitor. Hence the potential difference creates charge on each finger which is proportional to the applied voltage. The charge created causes a surface acoustic wave to be generated as a result of the piezoelectric effect. If we consider the first finger pair, the charge on the first finger creates a positive acoustic pulse and the charge on the second finger creates a negative pulse, hence creating an overall negative pulse. It can be seen that the second finger pair is connected to the busbar with an opposite sign to the first pair, so it will generate an overall positive pulse. It is clearly apparent that, by ordering the fingers in certain ways we can affect the creation of acoustic pulses. This effect is exploited in coding the devices as will be explained in later sections.

the code. For example, if the code (+ - + + -) is input into the IDT shown in figure 1, with the rightmost pulse first, each pulse would generate a positive SAW that will arrive at the receiver transducer and constructively interact. Because of that it is possible to produce a voltage that is significant enough to cause actuation [15].

Given that most IDT devices have the restriction of finger widths being $\lambda/4$ and finger pairs must be λ apart, so that constructive interference occurs, we can use the equation

$$\lambda = V/f, \quad (1)$$

where V is the velocity of the acoustic wave and f is the received transmission frequency, to design an IDT to receive any required frequency [16].

For example, if $V = 3500 \text{ m s}^{-1}$ as for lithium niobate and $f = 900 \text{ MHz}$, the finger pairs must be $3.8 \mu\text{m}$ apart and the finger widths must be $0.9 \mu\text{m}$ wide. From these fundamental restrictions we can calculate the number of finger pairs we can have, for a given valve size.

It should be noted that the fewer fingers an IDT has, the less precision it has in responding to a coded signal and the wider the bandwidth that will excite a surface acoustic wave [16]. The diameter of the human *vas deferens* is $400 \mu\text{m}$, hence for male fertility control applications this limits the total size of the valve, and thus the IDT would have to be smaller than this. That means a code length of 64 bits will require an IDT of $243 \mu\text{m}$. Further research is needed in this area to determine optimal input code lengths based on required

actuation voltage for a particular device and the proposed application.

Sensor devices work by reflecting back the SAW to the IDT for retransmission. This is achieved by using reflective plates on the polymer surface that return the SAW to the IDT. These reflectors, coupled with the attenuation through the polymer, enforce a constraint on the maximum size of the reply code to 32 bits. Any increase beyond this length results in the reflected SAW response being too small to be retransmitted [15].

One possible way to use the resulting device as a valve is to cut a slit into the polymer—as a SAW propagates through the substrate the slit will be periodically stretched and hence we have an oscillating aperture. When a fluid passes through the oscillating aperture its flow is restricted to a degree depending on its oscillation frequency. Hence, when a SAW is generated by the IDT with a frequency of 900 MHz , the flow will be severely restricted. However, this problem can be overcome, to a degree, by choosing a dielectric film for the polymer that has a high dispersive effect. This works by dispersing the travelling acoustic wave as it propagates along the polymer substrate. With current technology the wave can be transformed down to a frequency of 100 Hz , which only restricts the flow by a factor of 4, for a $400 \mu\text{m}$ aperture.

5. Structure of the microvalve and working principle

When the surface acoustic waves cause stresses in the polymer substrate, the resulting deflection can be of the order of microns [17], suggesting an ideal novel application would be a microvalve. Essentially, a small hole in the polymer substrate can be stretched to open wider or contracted by application of the RF signal on a SAW-on-polymer device. By sandwiching a number of these microvalves together, and by operating them in different phases, a peristaltic micropump could be created—this is very useful in cases where a fluid needs to be ‘pushed’ through the orifice. Alternatively, the SAW could be used to actuate a V-groove valve arrangement (also called a ‘check valve’). A further possibility is for passive venous valves (such as in artificial heart valves) to use the polymer device for monitoring the open/shut status of the valve, rather than for actuation. A host of lucrative applications from valves for electronic fertility control to micropumps for nanolitre drug delivery become foreseeable. The basic structure of the V-groove microvalve is shown in figure 4.

Three different polymer layers are utilized to create the valve:

- (i) UV curable structural polymer to form the body of the valve.
- (ii) A sacrificial polymer that can be etched away to leave cavities in the resulting 3D structure.
- (iii) A multifunctional polymer that has piezoelectrical properties that can act as either a SAW sensor or actuator.

The structural polymer, UV 001, is from HVS Technologies. It is a UV curable polymer with urethane acrylate, epoxy acrylate and acryloxysilane as the main ingredients. Its low viscosity allows easy processing through

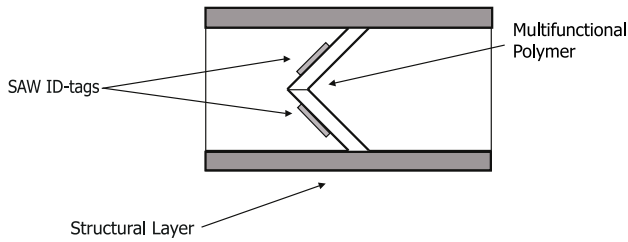


Figure 4. This figure shows the basic structure of a V-groove microvalve enhanced by SAW tags. It can be a passive valve or an active one. The passive microvalve can be opened or closed by the pressure of the surrounding fluid, depending on the direction of the fluid stream. In the case of a passive microvalve the SAW ID-tag electrodes have only the function of monitoring the status of the valve. That means that they are sending an RF signal to a reader station to give information about whether the valve is open or closed and where it is localized. But the microvalve can also be used as an active one. In this case the SAW ID-tag electrodes work as actuators, stretching open the polymer flaps with a cantilever action.

automatic equipment or manual methods without the addition of solvents or heat to reduce the viscosity. It also complies with all VOC regulations. It has excellent flexibility and resistance to fungus, solvents, water and chemicals. The sacrificial polymer is essentially an acrylic resin containing 50% silica. This composition can be dissolved with 2 mol l^{-1} caustic soda at 80°C . The multifunctional layer consists of nanoceramic particles attached by chemical bonding as side groups on a polymer backbone. The concept is a backbone with functional groups that will serve as anchor points for nanoparticle metal oxides. Nanoparticles such as PZT, PLZT, etc, must have active surfaces or functional groups that can bond with the polymer chain. The nanoparticles provide the piezoelectric function in the polymer and the backbone provides mechanical strength and structural integrity, electrical conductivity and other important properties. The backbone can be the same type of polymer as used for the structural layers. A new class of functional polymers have been synthesized at Pennsylvania State University, which can serve as the host for piezoelectric actuation.

6. Safety and reliability issues

There are many restrictions associated with RF technology that need to be considered. One of the main regulations is related to bandwidth and power dissipation. The relationship between the different frequency ranges and the maximum radiated power is shown in table 1. The Australian Communications and Media Authority (ACMA) releases licences for companies and strictly governs bandwidth and power emission. One of the main restrictions is on interference—devices must not cause interference to other radio communications services and must operate within the relevant ISM bands [16].

One of the fundamental concerns for RF *in vivo* applications is how the radiation affects the human body. Countless tests have been carried out researching a link between RF exposure and cancer. Hence a unit of measure called the specific absorption rate (SAR) has been developed. The SAR is the basic unit of measurement of RF fields between

Table 1. This table shows the maximum radiated power that is allowed to be sent through the human body at different frequency ranges [18].

Frequency band (MHz)	Maximum isotropically radiated power
915–928	1 W
2400–2463	4 W
2463–2483.5	20 mW
5725–5875	1 W

1 MHz and 10 GHz, with a SAR of 4 W kg^{-1} needed to produce adverse health effects. It has also been claimed that RF exposure induces heating in the body, which is thought to affect male fertility [11]. This is an area that needs to be investigated further. The maximum SAR is dependent on where in the body the device is placed so each application will have to verify the device is within these limits.

Neither the electric field (E) nor the magnetic field (H) penetrate far into a ‘good’ conductor. The point where the fields are reduced by a factor of $1/e \sim 1/2.71$ is called the electrical skin depth. Actuation forces (including external load) required for such a microvalve can be typically of the order of $100 \mu\text{N}$ [19] and moving through, say, a $10 \mu\text{m}$ displacement, corresponds to 1 nJ of energy.

Using the formula for the electrical skin depth given by

$$\delta = \sqrt{\frac{2}{\omega\sigma\mu}}, \quad (2)$$

where ω is the frequency in rad s^{-1} , μ the relative permeability and σ the conductance, we can see that for $f = 900 \text{ MHz}$ we have a penetration depth of 4.2 cm into human muscle or 3.9 cm into human skin [20]. That means that the antenna cannot be any further under the skin or muscle than these depths, if the signal is to be adequately received. It should be noted that the electrical skin depth is highly frequency- and material-dependent and hence will vary, depending on the context in which it is used.

For our calculations we assumed the worst case of 100 nJ of actuation energy required by the valve. The SAW device aperture can oscillate in the 10–100 Hz range, so we arbitrarily pick 50 Hz, for example. So the maximum delivered power of the antenna must be $20 \mu\text{W}$ for the 50 Hz example. From this we can work out the minimum power requirements through the air using the Friis equation:

$$P_R = P_T G_T G_R \left(\frac{\lambda}{4\pi R} \right)^2 \quad (3)$$

where G is the gain, R the distance and P the power of each antenna. We must also consider the attenuation of the power through the human skin and check that this is within the regulations. We also calculated the transmission through skin, and the penetration depth, attenuation and surface power of radio-frequency signals for skin and muscle at different frequencies. The results of those calculations are shown in table 2.

Table 2. This table shows the transmission of radio waves through skin, their penetration depth, attenuation and surface power for skin and muscle at different frequencies. It shows that the penetration depth in skin and muscle decreases with the increase of the frequency and that the attenuation of the body tissue and the surface power increase with an increase of the frequency used.

Frequency (MHz)	Transmission through skin (%)	Penetration depth (m)		Attenuation (dB)		Surface power (μW)	
		Skin	Muscle	Skin	Muscle	Skin	Muscle
434	26.9	0.0551	0.0525	0.119	0.128	76.1	75.45
920	26.5	0.0396	0.0417	1.37	1.18	88.4	86.5
2450	27.8	0.0224	0.0221	1.42	2.36	84.7	94.4

Table 3. This table shows sizes and properties of simple dipole antennas at different frequencies.

Operating frequency (MHz)	Antenna size (cm)	Antenna length (cm)	Wave length (cm)	Efficiency (%)	Far field (μm)	Transmitted power (μW)	Inside regulations
434	1	$\lambda/69$	69	96	290	29.12	Y
920	1	$\lambda/33$	33	99	606	147.5	Y
2450	1	$\lambda/12$	12	99.8	1670	995	Y
434	0.5	$\lambda/138$	69	92	72	30.4	Y
920	0.5	$\lambda/66$	33	97	151	146	Y
2450	0.5	$\lambda/24$	12	99.9	417	994	Y
434	0.25	$\lambda/69$	69	86	19	32.6	Y
920	0.25	$\lambda/69$	33	94	38	155.4	Y
2450	0.25	$\lambda/69$	12	98	104	1014	Y

The attenuation of the body tissue was calculated by the following equations:

$$A = e^{(-|\Im(\beta)|d)} \quad (4)$$

$$\beta = \frac{\omega}{c} \sqrt{1 - \frac{j\sigma}{2\omega\epsilon}}, \quad (5)$$

where the attenuation is a term in solution of the wave equations, ω the frequency in rads s^{-1} , c the velocity of light, σ the conductivity and ϵ the permittivity of the medium. Because the conductivity and permittivity are highly frequency- and material-dependent, the values will vary, depending on the context in which they are used [21]. We assumed $d = 5$ cm for the distance between the transmit and receive antennas.

Since $\frac{\sigma}{\omega\epsilon}$ is small, we can use a Taylor approximation to give

$$\beta = \omega/c \left(1 - \frac{j\sigma}{2\omega\epsilon} \right). \quad (6)$$

To make the relationship between the antenna size, width and efficiency at different frequencies clearer, we calculated the values shown in table 3 by the following equations.

We calculated the efficiency by using the basic equation for short dipole antennas:

$$\eta = \frac{R_{\text{rad}}}{R_{\text{ohm}} + R_{\text{rad}}} \quad (7)$$

$$R_{\text{rad}} = 80 \left(\frac{\pi l}{\lambda} \right)^2 \quad (8)$$

$$R_{\text{ohm}} = \frac{lR_s}{3\pi a} \Rightarrow R_s = \frac{1}{\delta\sigma}, \quad (9)$$

where l is $1/2$ length of the dipole, a the radius of the antenna of 1 mm, R_s the surface resistance of the material and δ

the electrical skin depth. We also assumed a gain of the transmitting antenna of 1.5 and $\sigma = 4.1 \times 10^7 \text{ S m}^{-1}$ for typical antenna metal (gold).

Initial research suggested the efficiency of the proposed antenna would be quite low and this would make the required transmit power exceed the regulations, which would make the construction of the devices untenable. However, after the calculations it can be seen that the efficiency remains quite high, because the antenna thickness (1 mm) is reasonably large compared to the antenna length (1 cm). From this we can see that using an antenna of this size is a viable solution to meet the required specifications. To make that more clear we calculated the antenna size and length for different frequencies and also the efficiency and the transmitted power. The results of those calculations are shown in table 3.

There are several design techniques that may allow us to design an antenna that is small enough. Some of the most currently common methods include using a meander antenna [22]. Further design methods include fractal antenna design, which is the process of minimizing the area of a square loop using fractal shapes. This allows the loop to be at least four times smaller than non-fractal designs, for comparable efficiency [23]. A fractal antenna approach also allows a smaller resonant frequency to be used compared with an ordinary approach. This means that a larger receiving area can be fitted into the same size, which increases the overall power received [24]. One of the current methods for fractal approaches uses Hilbert curves [25]. A comparison between a dipole and a Sierpinski fractal antenna is shown in figure 5.

7. Applications

This section describes some of the main biomedical fields in which the RF-controlled microvalve may be applied, i.e.

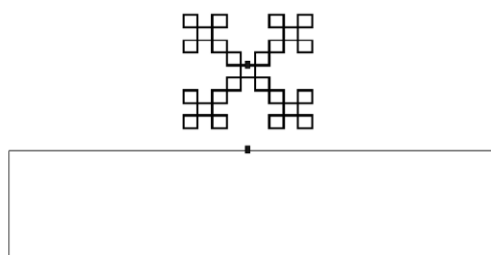


Figure 5. This figure shows a schematic comparison of two folded dipoles. The top one is an efficient Sierpinski fractal loop about 1/4 the area of the loop (below), with virtually the same gain [23].

- (1) fertility control, (2) drug delivery, (3) flow cytometry and (4) DNA sequencing.

7.1. Fertility control

There are a variety of methods for conception control such as using the ‘pill’ or performing a vasectomy. But the choice of a suitable method is very difficult and the potential risks and benefits must be carefully analysed [26]. For example there are many side effects to using the ‘pill’ and a vasectomy reversal has a high failure rate containing a painful surgical procedure with an inconvenient recovery time for the patient [27]. To avoid these problems the microvalve described above could be used. It could be placed in the *vas deferens* of a male to make restored fertility possible and relatively easy. Within the first two weeks after insertion, the valve can be episodically switched on and off, reducing the backpressure during the early stages when the valve adheres to the walls of the *vas deferens* and to reduce any possible build up of proteins on the face of the valve. The insertion can be performed by a hypodermic needle [28].

We are unable to insert the microvalve in the female ovarian duct because the ovarian duct has an inner surface which is coated with *microvilli* that are like microscopic fingers which help the *ova* to move along the duct in the correct direction. The ovarian duct is also very sensitive to foreign objects which tends to cause adhesion within the tube [28].

7.2. Drug delivery

In many different cases it is very useful if drugs can be delivered at the right time and as close to the treatment area as possible [29], such as, for example, in the case of *diabetes mellitus*. To make this possible, drug delivery micropumps that can be implanted in the body are used to deliver small quantities of drug from a reservoir. These micropumps would avoid the strain on veins of weekly or daily injections. In this case, an RF-controlled microvalve could be integrated in an implanted drug delivery system and make it possible to set the correct drug dosage to be applied at the right time [30]. Existing approaches either use an osmotic valve, which unfortunately provides a continuous feed, or have the disadvantage of battery power.

7.3. Flow cytometry

The basis of flow cytometry is that specific optical characteristics (such as fluorescence or light scatter) can

provide a measure of the specific physical or chemical properties of biological particles (such as size and DNA content). The principle of flow cytometry has been integrated into a micromachined silica flow chamber [31]. In this instrument a collection of small particles is pumped through a specially designed transparent tube. A measurement is made when the particles pass the ‘sensing region’. This region is delimited by the illumination and collection regions which are provided by light source and optical detector assemblies.

The RF-controlled microvalve could be integrated into a flow cytometry system to control the stream of particles, which would keep the biological cells of interest in a separate particle chamber for later investigations. It could also prevent a reverse flow of the cells out of this chamber [30].

7.4. DNA sequencing

Present DNA sequencing methods employ electrophoresis and they are still quite slow and expensive. To speed up the sequencing process and reduce costs through miniaturization, one idea is to pull a strand of DNA through a tiny hole in a polymer material immersed in an ion solution [32]. Variations of the ion current are detected, which correspond to the A, G, C or T bases in the DNA molecule. One key problem is that of poor signal-to-noise ratio (SNR) in the measured current. The proposed SAW-on-polymer devices provide a means to adaptively modulate the diameter of the hole to optimize the SNR via use of lock-in amplifier techniques.

8. Fertility control modelling study

The microvalve which can be employed for fertility control or to replace a vasectomy is shown in figure 6. The main element of the valve is the multifunctional polymer actuator, which serves at the same time as a closure element of the microvalve. The wireless communication principle via ID tag is used as previously described. The ID tag is deposited on the surface of the polymer actuator. The corresponding reader/transmitter station is outside the human body. The valve is closed in the initial state if no RF signal is sent to the ID tag. In this state, infertility is set. If a sperm or *ovum* should pass through the microvalve, RF pulses are transmitted by the base station, which is located outside the body, to the valve. Because of the deformation of the actuator material, the microvalve opens and closes with a certain frequency, which depends on material damping and the metal electrode configuration on the SAW device. Static opening is difficult, so the intention is to develop a device in which the orifice opens cyclically at a certain frequency. The lower the frequency, the more severe the demands on the RF power to the device. On the other hand, as will now be examined, there are fluid-dynamic restrictions on how high the frequency can be.

So, let us now consider the possible simplifications for modelling the fluid flow through the oscillating orifice. The orifice must not vibrate so fast that one sperm cannot get through in one cycle—this restriction can be defined by a Strouhal number. To get an idea of the sizes we are talking about, the head of a typical human sperm has a length

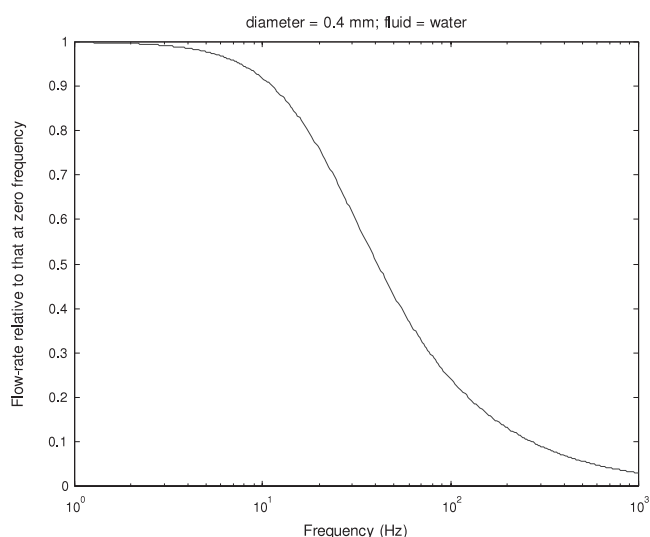


Figure 6. Normalized flow rate versus frequency of valve switching. As the orifice frequency increases from 1 to 1000 Hz, the impedance to one-way aqueous flow rises, such that normalized flow rate is reduced to 10% or less above 250 Hz.

of 5–6 μm , the diameter (width) is 2.5–3.5 μm and the width/length ratio is 1/2–3/5 [33]. There is also the possibility of damage to the sperm. The achievable rate will also drop dramatically when the opening is loaded by surrounding fluid. The situation has some similarity to that of a vibrating diaphragm for a pressure transducer; the natural frequency goes down by at least two orders of magnitude when a liquid-filled catheter is connected. Alternatively, if the valve were so powerful that it vibrated without being slowed down by the fluid, it would at some frequency cavitate the fluid, with disastrous effects on valve longevity and (again) degree of sperm damage. This effect is well known from ultrasonic frequencies at therapeutic power levels.

For the purposes of initial analysis of the problem, one can ignore geometric details and examine, for instance, an oscillating aperture. However, even that simplification poses a spectrum of possibilities between, on the one hand, a hole time-varying radius in a wall of negligible thickness and, on the other, a long pipe of time-varying radius through a very thick wall. These present completely different difficulties for fluid flow.

Therefore a still further level of simplification is addressed. The approach is to think of this interrupted flow (geometry unspecified, but a zero-thickness shutter is probably closest in spirit) as having to accelerate from zero every time the shutter opens, under the action of the prevailing pressure gradient as set by whatever pressures are exerted upstream and downstream. On this basis the flow is not unlike the situation of a purely oscillatory flow in a pipe, under the influence of a sinusoidal pressure gradient. The assumed flow is then laminar and Newtonian, and takes place far from the ends of a straight pipe. This is a standard problem, for which the solution was provided by Womersley (1957) [34, 35]. Inserting the fluid properties (density and viscosity of water) and tube diameter of the *vas deferens* (0.4 mm internally) leads to the result shown

(figure 6). The result may favorably err on the conservative side, in that there is no allowance for the elastic storage of energy in the vessel wall upstream of the shutter when it closes.

The decline of oscillatory flow rate with frequency indicates that, despite the small tube diameter, in the frequency range of interest the situation is far from being purely Stokes flow; momentum plays a highly significant role in determining the flow that occurs in response to the applied pressure gradient. In the present context, what is here determined is the extent of forward flow for a given frequency of opening orifice, relative to the flow that would occur through the tube if the microvalve presented no obstruction at all by periodic closure. It is also assumed that no partial obstruction of the tube occurs when the microvalve is open.

The fluid dynamic simulation has a typical low pass characteristic with a cutoff frequency f_c of 30 Hz. The frequency range of interest here is between 10 and 100 Hz. In that particular range, the flow rate relative to that at 0 Hz is 90% for 10 Hz and 25% for 100 Hz. From the physiological point of view, the flow rate at 100 Hz is sufficient for sperm transport through the microvalve, whereas it is desirable to have a higher flow rate. The flow simulation shows that a material is needed which is able to oscillate in that frequency range. Oscillations at such low frequencies are achieved by a special arrangement and distances of electrodes on the surface of the SAW device and by the fact that the nanoparticle-embedded polymer is a highly damped material. Frequencies down to 100 Hz have been achieved at Penn State and work is ongoing for further reduction.

9. Open questions and future work

We considered a number of application areas for an RF-controllable microvalve in this paper. In new fields of research, there are many questions to be answered before any invention can be safely applied. Above all, in the field of fertility control it is important to make sure that the microvalve works correctly and efficiently to prevent problems which could endanger the patient. Considering the expansion of the actuator material, analysis should also be done if a particular shape of the microvalve has an influence on the displacement of the actuator material. It is not yet known whether there exist differences in displacement of different shapes of the valve. The aim is to find the 'optimum' shape which satisfies the requirements of displacement for application in the area of fertility control. Furthermore, it should be established which shape is the easiest to implant in the body in order to prevent complications in surgery and additional pain for the patient. Initially, these tests, together with tests for the functionality of the valve, can be undertaken in animals such as sheep or pigs. Apart from that point of view, there is also room for electromechanical modelling of the actuator material of the valve. In particular, the gain of the antennas versus the suitable frequency ranges has to be carefully analysed. In this paper we discussed a rough survey of the frequencies and the power densities which are allowed to be used. The next step in research is to analyse the efficiency of the antenna, because the lower the RF frequency, the lower the gain of the antenna, which makes it difficult to

deliver enough power to cause a certain amount of strain in the material. In this study we only considered a simple dipole antenna structure. Improved trade-offs between efficiency and antenna size may be achieved by use of other geometries such as fractal antennas [36]. For a given frequency, suboptimal small antennas may be possible at the expense of increased external RF power—the limit to this trade-off will depend on the safety requirement for transcutaneous RF transmission for each given application. Given that the human *vas deferens* is of the order of 400 μm in diameter, male fertility control is a rather ambitious goal, as the whole integrated valve would have to fit into that diameter. Therefore our near-term goal will be to firstly target drug-delivery applications, where the size restriction can be greatly eased. Size requirement will impact on the lowest usable RF frequency, and in this programme we will push valve size and antenna size down as far as we can go to find the limits. The ultimate goal of a 400 μm size for male fertility control is not untenable, however. To achieve this would require a high dielectric layer on a chiral absorber, using a fractal microantenna approach. Note also that the space saving by using the Sierpinski fractal approach of Puente [36] has recently been surpassed by using a Hilbert curve fractal [25]. Although bringing the concept of the Hilbert fractal antenna together with the chiral absorber is beyond the scope of this paper, we will examine its feasibility in the future. Another question is whether the SAW device can exert the forces required to control flow against ultimately physiological pressure gradients. In the short term, the proposed device will simply be limited to a narrow range of applications, if higher pressure gradients prove problematic. In the longer term, new polymer substrate materials may emerge (e.g. nanotube-embedded polymer) that exhibit higher actuation strains. The aim of material simulations is to find a material which needs a very low energy level to cause a relatively high deformation. The frequency behaviour of the material could be calculated by a simulation of the valve. Together with a simulation of the different shapes of microvalves, we can optimize the microvalve set-up for fertility control. As a result of these simulations, a first model could be constructed following the required design specifications. In modelling the SAW device, different acoustic modes need to be analysed for example, one would expect horizontal shear modes to be more useful than Rayleigh modes. This is because when a SAW device is *in vitro*, Rayleigh modes are rapidly damped out. Horizontal mode polymer devices have been devised at Pennsylvania State University—these are manufactured by pulling the polymer melt through a field, so that the piezoelectric nanoparticles polarize and align in the preferred direction for horizontal mode propagation.

10. Conclusion

In this paper an RF-controllable microvalve for medical applications was discussed. By using wireless communication and surface acoustic wave devices, a valve can be devised for implantation into a section of the *vas deferens* that occurs just after the *epididymis*. The implantation can be carried out by use of a hypodermic needle.

For implantation the valve material has to be compatible with the human body. The microvalve which is described in this paper consists of silicone-based polymers, which are expected to be biocompatible. In principle, the biocompatibility issue can in future be further addressed by use of dacron or biopolymer silicone coatings on the valve.

The working principle of the microvalve is based on the previously described SAW concept in which a reader/transmitter station (outside the body) sends RF pulses to an ID tag (inside the body), which is printed on the actuator of the valve. These RF pulses are received by the ID tag of the valve and converted into surface acoustic waves (SAWs). The SAWs propagate along the surface of the piezoelectric actuator and cause the required alternating deflection which is used to open and close the valve at a certain frequency.

We also discussed the encoding of SAW devices, which is very important for successful *in vivo* applications. We can achieve encoding of SAW devices by using the IDT's fingers in a specific order. Their polarity and orientation would be related to the input code and we could ensure that only the correct acoustic wave propagates. The maximum code length of reply is restricted at the moment to 32 bits.

We have determined that the efficiency of the proposed antenna is quite high, because the antenna thickness of 1 mm is reasonably large compared to the antenna length of 1 cm. From this one can see that using an antenna of this size would be a viable solution to meet the required specifications.

The fluid dynamic behaviour of the microvalve was discussed in the case study for the fertility control application, where the flow rate through the oscillating valve aperture has a low-pass characteristic. The frequency range of interest is between 10 and 100 Hz. These frequencies are achieved by a special arrangement of surface electrodes on the actuator material of the valve and arranging suitable acoustic dispersal in the polymer. So far acoustic frequencies as low as 100 Hz have been achieved at Pennsylvania State University. The flow rate of sperm through the microvalve still obeys physiological requirements for the fertilization of the human *ovum* in the frequency range of 10–100 Hz. The flow rate in this range relative to the flow rate of 100% at 0 Hz is 75% at 100 Hz and only 10% at 10 Hz.

Acknowledgments

The authors would like to thank all members of both the Department of Electrical and Electronic Engineering and the Centre of Biomedical Engineering at the University of Adelaide for their helpful support.

References

- [1] Johnson A D and Shahoian E J 1995 Recent progress in thin film shape memory microactuators *IEEE Micro Electro Mech. Syst. Workshop* pp 216–20
- [2] Benecke W 1991 Silicon microactuators: activation mechanisms and scaling problems *6th Int. Conf. on Solid-State Sensors and Actuators* pp 46–59

- [3] van de Pol F C M, van Lintel H T G, Elwenspoek M and Fluitman J H J 1990 A thermopneumatic micropump based on micro-engineering techniques *Sensors Actuators* **21** 198–202
- [4] Boehm S, Olthuis W and Bergveld P 1999 An electrochemically actuated micropump for use in a 'push-pull' microdialysis based *in vivo* monitoring system *10th Int. Conf. on Solid-State Sensors and Actuators* pp 880–1
- [5] Trimmer W S N, Gabriel K J and Mahadevan R 1987 Silicon electrostatic motors *4th Int. Conf. on Solid-State Sensors and Actuators* pp 857–60
- [6] Wagner B, Kreuzer M and Benecke W 1992 Linear and rotational magnetic micromotors fabricated using silicon technology *Proc. IEEE Micro Electro Mech. Syst.* **183–9**
- [7] Robbins W P, Polla D L, Tamagawa T and Glumac D E 1991 Design of linear-motion microactuators using piezoelectric thin films *J. Micromech. Microeng.* **1** 247–52
- [8] Que L, Park J S and Gianchandani Y B 1999 Bent-beam electrothermal actuators for high force applications *IEEE Micro Electro Mech. Syst.* 31–6
- [9] Reynaerts D, Peirs J and van Brussel H 1997 An implantable drug-delivery system based on shape memory alloy micro-actuation *Sensors Actuators* **61** 455–62
- [10] Quandt E and Seemann K 1995 Fabrication and simulation of magnetostrictive thin film actuators *Sensors Actuators* **50** 105–9
- [11] de Leeuw D 1999 Plastic electronics *Phys. World* **12** 31–4
- [12] Bonomo C, Fortuna L, Giannone P, Graziani S and Strazzeri S 2006 A model for ionic polymer metal composites as sensors *Smart Mater. Struct.* **15** 749–58
- [13] Bonomo C, Fortuna L, Giannone P, Graziani S and Strazzeri S 2006 A nonlinear model for ionic polymer metal composites as actuators *Smart Mater. Struct.* **16** 1–12
- [14] Ruppel C W and Fjildly T 2000 *Advances in SAW Technology, Systems and Applications* vol 1, pp 1–3
- [15] Schmidt F, Sczesney O, Ruppel C and Magori V 1996 Wireless interrogator system for saw-identification-marks, and saw-sensor components *IEEE Int. Frequency Control Symp.* **96CH35935** 208–15
- [16] Australian Communications and Media Authority http://www.acma.gov.au/WEB/STANDARD/pc=PC_481
- [17] Varadan V V, Varadan V K and Bao X Q 1998 IDT sensors for detection of ice on rotorcraft *Proc. SPIE Smart Struct. Mater.: Smart Electronics and MEMS* **3328** 49–58
- [18] International Commission on Non-Ionizing Protection (ICNIRP) 1998 Guidelines for limited exposure to time-varying electric, magnetic, and electromagnetic fields (up to 300 GHz) *Health Phys.* **74** 494–522
- [19] Kohl M, Gottert J and Mohr J 1996 Verification of the micromechanical characteristics of linear actuators *Sensors Actuators* **53** 416–22
- [20] Gabriel C 1996 Compilation of the dielectric properties of body tissues at RF and microwave frequencies *Report N.AL/OE-TR-1996-0037*, Occupational and Environmental Health Directorate, Radiofrequency Radiation Division
- [21] Italian National Research Council, Institutes of Applied Physics <http://www.ifac.cnr.it/>
- [22] Varadan V K, Varadan V V and Bao X Q 1996 Integration of interdigital transducers, MEMS and antennas for smart structures *Proc. SPIE Smart Struct. Mater.: Smart Electronics and MEMS* **2722** 95–106
- [23] Vernon T 1999 Fractal antennas offer benefits *Radio World* <http://www.hbc.com/~wenonah/cfa/fractal.htm>
- [24] Varadan V K and Gardner J W 1999 Smart tongue and nose *Proc. SPIE Smart Struct. Mater.: Smart Electronics and MEMS* **3673** 67–76
- [25] Vinoy K J, Jose K A, Varadan V K and Varadan V V 2001 Hilbert curve fractal antenna: a small resonant antenna for VHF/UHF applications *Microw. Opt. Technol. Lett.* **29** 215–9
- [26] Martini F 1992 *Anatomy and Physiology* 2nd edn (Englewood Cliffs, NJ: Prentice-Hall) chapter 21, 28, pp 669, 950
- [27] Fisch H 2007 Male infertility http://www.cumc.columbia.edu/dept/urology/MaleInfertility_reversal.html
- [28] Moffett D 1993 *Human Physiology: Foundations and Frontiers* 2nd edn (St Louis, MO: Mosby-Year Book) chapter 24, p 688
- [29] Dario P, Carrozza M C, Benevenuto A and Menciassi A 2000 Microsystems in biomedical applications *J. Micromech. Microeng.* **10** 235–44
- [30] Enderling S, Varadan V K and Abbott D 2001 Directions for RF controlled intelligent microvalve *Proc. SPIE Smart Electron. MEMS* **4236** 204–12
- [31] Sobek D, Senturia S D and Gray M L 1994 Microfabricated fused silica flow chambers for flow cytometry *Solid-State Sensors and Actuators Workshop* pp 260–3
- [32] Kasianowicz J, Brandin E, Branton D and Deamer D 1996 Characterization of individual polynucleotide molecules using a membrane channel *Proc. Natl Acad. Sci.* **93** 13770–3
- [33] Kruger T F, Acosta A A, Simmons K F, Swanson R J, Matta J F and Oehninger S 1988 Predictive value of abnormal sperm morphology in *in vitro* fertilization *Fertil. Steril.* **49** 112–7
- [34] Womersley J R 1957 An elastic tube theory of pulse transmission and oscillatory flow in mammalian arteries *Tech. Rep.* TR56-614, Aeronautical Research Laboratory Wright-Patterson Air Force Base
- [35] Womersley J R 1957 Oscillatory flow in arteries: the constrained elastic tube as a model of arterial flow and pulse transmission *Phys. Med. Biol.* **2** 178–87
- [36] Puente C, Anguera J, Borja C and Soler J 2001 Fractal-shaped antennas and their application to GSM 900/1800 *J. Inst. Br. Telecom. Eng.* **3** 2 92–5